Living in a swampy paradise: Paleoenvironmental reconstruction of an African Humid Period lacustrine margin, West Turkana, Kenya

Article · March 2019

DOI: 10.1016/j.jafrearsci.2019.03.007

Journal of African Earth Sciences 154 (2019) 20–34

Contents lists available at ScienceDirect

Journal of African Earth Sciences

journal homepage: www.elsevier.com/locate/jafrearsci

Living in a swampy paradise: Paleoenvironmental reconstruction of an African Humid Period lacustrine margin, West Turkana, Kenya

Catherine C. Beck*, Mary Margaret Allen, Craig S. Feibel, Emily J. Beverly, Jeffery R. Stone, Bruce Wegter, Charles L. Wilson IV

Hamilton College, USA

ARTICLE INFO

Keywords:
Turkana
African humid period
Wetland resources
Galana Boi
Holocene
Paleoenvironmental reconstruction

ABSTRACT

The African Humid Period (AHP), spanning ~15-5 ka, was characterize across East Africa by increased precipitation. Wetter climate conditions created environments favorable to human occupation in what are today harsh, resource-limited places to inhabit. The Turkana Basin is a striking example of this. Throughout the AHP, lake levels intermittently rose ~100 m establishing hydrologic connectivity from Lake Turkana into the Nile drainage system via an outlet to the northwest. This study presents new, high-resolution data from West Turkana outcrops of the Late Pleistocene/Holocene Galana Boi Formation. This research complements existing lake-level curves and allows for landscape reconstruction through lateral facies associations. The Kabua Gorge area contains both well-exposed stratigraphic sections and multiple archaeological sites to the north and west of the outcrops. This creates the opportunity to tie the archaeology closely to paleoenvironmental reconstructions from the geological record. The depositional environment is characterized by a dynamic fluctuating lake margin, consisting of at least four phases of inundation. Highstand Phase 4 is distinct within the Kabua Gorge sequence because it is comprised of black clay containing 2–10% total organic carbon, pedogenic overprinting, pedogenic carbonate nodules, and a diverse molluscan fauna. Deposition of this unit is indicative of an organic-rich, reducing lacustrine environment that was subsequently overprinted by pedogenesis. This unit grades laterally basinward from organic-rich paleosols to lacustrine silts characterized by abundant freshwater diatom taxa. By coupling sedimentology, diatom assemblage data, $\delta^{13}C$ and $\delta^{18}O$ isotope geochemistry of pedogenic carbonates, and a radiocarbon chronology for the area, the paleoenvironment of Kabua Gorge is interpreted as a shallow marshy embayment connected to the main body of a freshwater Lake Turkana. The landscape is a highly dynamic one, varying on a scale of 100s of meters. Sediments were deposited during periods of inundation and then pedogenically modified during brief periods of subaerial exposure to form Vertisols. Archaeological sites in the early part of the AHP at Kabua Gorge are closely associated in age with lacustrine highstands. Hence, we propose that the lagoonal marsh environment of Phase 4 would likewise have been a resource-rich area for human occupation during the AHP. Potential resources drawing humans to the area include access to fresh water and fishing grounds. Ultimately, understanding the paleoenvironmental dynamics at Kabua Gorge provides a window into the broader ecosystems in which humans culturally evolved from the Late Pleistocene to present.

1. Introduction

The African Humid Period (AHP) shaped the landscape in which *Homo sapiens* evolved culturally over the last ~14 ka in the Turkana Basin of northern Kenya and across Africa. An increase in solar insolation driven by Milankovitch cycles, specifically half precession, increased the intensity of the East African monsoon by up to 17% (Kutzbach and Liu, 1997). This created climatic conditions across East Africa that were significantly wetter than today (Kutzbach, 1981). While the timing of onset, and particularly the termination, of AHP is time-transgressive across Africa (Shanahan et al., 2015), it dramatically impacted the paleoenvironment and the ecosystems that depend upon it. At the start of the AHP in this region (~14 ka) (Beck, 2015), Lake Turkana rose ~100 m higher than modern levels, overflowing into the Nile drainage through a spillway located in the northwestern margin of the lake (Garcin et al., 2012; Morrissey and Scholz, 2014). For humans living in the region, the AHP highstands created new opportunities for resource acquisition in marginal lacustrine environments that are

* Corresponding author.
E-mail address: ccbeck@hamilton.edu (C.C. Beck).

https://doi.org/10.1016/j.jafrearsci.2019.03.007
Received 12 November 2018; Received in revised form 9 March 2019; Accepted 11 March 2019
Available online 18 March 2019
1464-343X/

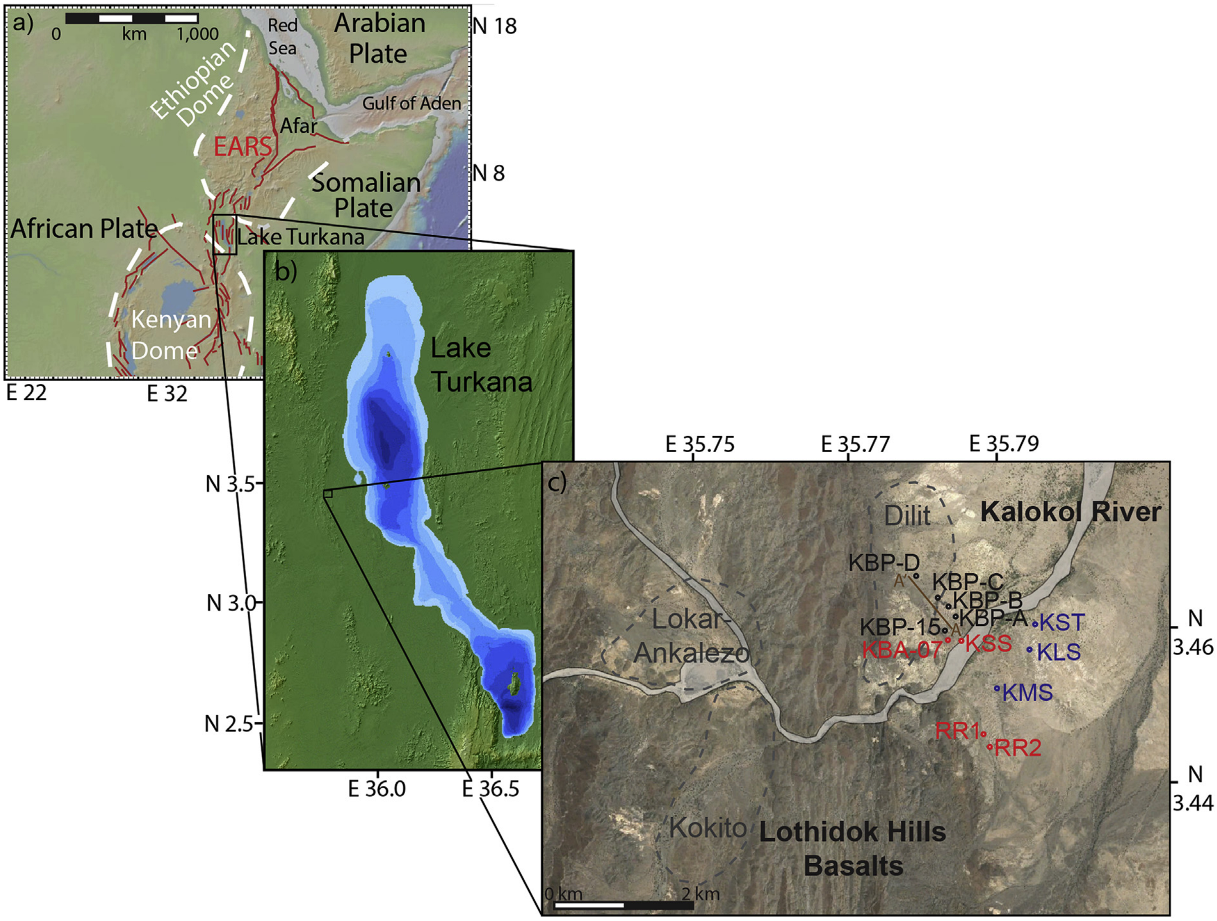

Fig. 1. a) DEM of East Africa with major East African Rift System (EARS) faults in red and structural domes outlined with dashed white lines. b) DEM of the modern Lake Turkana showing the study area. c) Kabua Gorge study area showing Dilit, Kokito, and Lokar-Ankalezo archaeological sites (Beyin et al., 2017). The Miocene Lothidok Hills Basalts, oriented N-S through the study area, create a topographic highpoint and the incision of the Kalokol River through them creates the Kabua Gorge. Position of stratigraphic sections and sample localities noted, with sections presented in Beck (2015) in red, new sections shown in blue, and paleosol sections in black. Transect (A′ to A) presented in Fig. 9 shown in brown.

preserved well above the modern lake (Wright et al., 2015). This includes archaeological evidence of fishing (Whitworth, 1965a; Beyin, 2011; Beyin et al., 2017) and evidence of warfare (Mirazon Lahr et al., 2016), which may point to resource-rich localities that were worth risking bodily harm to protect from rival groups (Marean, 2011).

This study focuses on a ~4 km^2 area of exposure termed Kabua Gorge (Whitworth, 1965b), located near the western shore of Lake Turkana, ~12 km southwest of the village of Kalokol (Fig. 1). While the name Kabua is a misnomer for the local name Kapua, it is used here as Kabua continues to be regularly associated with the locality and its ties to the published literature. Here the Kalokol River cuts through a ridge of the Miocene Kalokol basalts (Boschetto et al., 1992). Kabua Gorge preserves an extensive section of the Late Pleistocene to Holocene Galana Boi Formation. Originally described and designated from Koobi Fora on the east side of Lake Turkana (Owen and Renaut, 1986), the Galana Boi Formation and its lateral equivalent, Kibish Formation Member IV in southern Ethiopia (Brown and Fuller, 2008), contain multiple archaeological sites (Robbins, 1975; Barthelme, 1977, 1985; Owen et al., 1982; Ashley et al., 2011; Beyin, 2011; Foerster et al., 2015; Mirazon Lahr et al., 2016; Goldstein et al., 2017). The Galana Boi sediments basin-wide have undergone minimal structural modification since their deposition (Owen and Renaut, 1986; Garcin et al., 2012), supporting the assumption they are in their original orientation. From a paleoenvironmental perspective, they record the response of Lake Turkana to increased moisture associated with the AHP during the Late Pleistocene through to the Middle Holocene (~7 ka) when the accommodation space in this part of the basin filled and the lake regressed. Due to the highly dynamic nature of the environment it preserves, the Galana Boi Formation at Kabua Gorge is difficult to characterize with one section. However, the Late Pleistocene to Early Holocene sedimentation is typified by three previously recognized lacustrine intervals (Phase 1, 2, and 3), which are dominated by thinly-bedded to laminated silts (Beck, 2015). The record from Kabua Gorge is based upon seven stratigraphic sections and the geochemical records preserved in them (Fig. 1).

The study area is directly associated with the archaeological sites of Kokito, Dilit, and Lokar-Ankalezo (Beyin, 2011; Beyin et al., 2017). Previous work has demonstrated the importance of Kabua Gorge and the associated sites of Dilit and Kokito to the archaeological record (Whitworth, 1965a; Beyin, 2011; Bloszies et al., 2015). In particular, radiocarbon dates from two sites within the Kokito area demonstrate that humans inhabited the area at least periodically from ~14 to 9 ka (Table 1). The archaeofaunal evidence from these sites includes abundant fish remains and evidence of fishing technology in the form of barbed points (Beyin et al., 2017). Across the East African Rift System and the Sahelian zone, AHP communities exploited fish as part of their subsistence strategy (Stewart, 1991). Recognition of aquatic resources lead to the designation of hunter-gatherer-fisher communities across the African continent and within the Turkana Basin specifically (Robbins, 1974; Prendergast and Beyin, 2018; Chritz et al., 2019). Additionally, fish are not the only aquatic resource used by humans during this period as archaeofaunal evidence suggests these

Table 1
Radiocarbon dates from this study, Beck (2015), and van der Lubbe et al. (2017), and Beyin et al. (2017). Final Age (cal BP) is the mean of the Calibrated results (2 sigma). Elevations are rounded to the nearest meter.

Reference	Sample #	Lab ID	Location	Material	Measured Age (BP)	δ13C (per mil)	Calibrated result (BP)	Final Age (cal BP)	Elev (m)
this study	15-KBA-07	420650	KSS	mollusc	6020 ± 30	−0.3	7425–7275	7350 ± 75	450
this study	16-KLS-14	445593	KLS	mollusc	7070 ± 30	−1.4	8365–8195	8280 ± 85	426
Beck (2015)	Kabua 02-01	402648	Charcoal Section	charcoal	9410 ± 30	−26	10695–10560	10630 ± 140	420
Beck (2015)	Kabua 02-02	402649	Charcoal Section < 4 cm below charcoal	mollusc	9280 ± 30	−3.3	11175-11070 10955-10865 10850-10805	10990 ± 190	420
van der Lubbe et al. (2017)	Kabua179-A	3775179	KSS	charcoal	9530 ± 40	−24.4	11085-10920 10890-10705	10900 ± 190	418
van der Lubbe et al. (2017)	Kabua 30	396299	RR1	mollusc	9790 ± 40	−4.1	11970-11610 11520-11510	11740 ± 230	445
van der Lubbe et al. (2017)	Kabua 26	396300	RR1	mollusc	10790 ± 40	−2.4	13090–12990	13040 ± 50	442
van der Lubbe et al. (2017)	Kabua 22a	396301	RR1	mollusc	11670 ± 40	−4.4	13980–13755	13870 ± 120	438
Beyin et al. (2017)		A3724	Kokito 02	charcoal	11735 ± 30	−27	13610–13450	13530 ± 80	437
Beyin et al. (2017)		A3723	Kokito 02	charcoal	11670 ± 25	−25	13565–13440	13503 ± 62	437
Beyin et al. (2017)		A3720	Kokito 02	charcoal	11705 ± 25	−25	13575–13455	13515 ± 60	437
Beyin et al. (2017)		A3028	Kokito 02	charcoal	11670 ± 35	−26	13570–13435	13503 ± 67	437
Beyin et al. (2017)		A3752	Kokito 01	charcoal	14745 ± 50	−17	18110–17760	17935 ± 175	447
Beyin et al. (2017)		A3753	Kokito 01	mollusc	9710 ± 35	−5.9	11220–11085	11153 ± 67	447
Beyin et al. (2017)		A1715	Kokito 01	charcoal	9060 ± 30	−24	10245–10190	10218 ± 27	447
Beyin et al. (2017)		A3721	Kokito 01	charcoal	9600 ± 25	−24	11125–10775	10950 ± 175	447
Beyin et al. (2017)		A1714	Kokito 01	charcoal	9785 ± 35	−25	11245–11175	11210 ± 35	447
Beyin et al. (2017)		A3722	Kokito 01	charcoal	11530 ± 25	−26	13440–13295	13368 ± 72	447
Beyin et al. (2017)		A3754	Kokito 01	mollusc	10825 ± 40	−3.9	12765–12680	12723 ± 42	447

communities also processed water birds, turtles, crocodile, and even hippopotamus (Prendergast and Beyin, 2018). These studies emphasized the importance of aquatic resources as part of the subsistence strategy for Late Pleistocene to Holocene populations.

Access to fresh water is another essential resource required by humans. However, being proximal to a lake is not a guarantee that potable water is present. Modern Lake Turkana is alkaline (pH 9.2) and moderately saline (TDS = 2500 ppm) putting it at a critical extinction threshold for molluscs and at the upper level for many common fish species (Yuretich and Cerling, 1983). However, during the Holocene when Lake Turkana overflowed into the Nile drainage basin, the lake freshened making it more hospitable to both humans and the aquatic ecosystems they depended upon. There is evidence that this overflow may have first occurred as early as 11.7 ka (Beck et al., 2019) and during the span of time investigated by this study the lake waxed and waned between overflow and balanced or underflow conditions. This study builds upon the existing local and basin-wide archaeological framework to offer a coupled terrestrial and aquatic reconstruction of the landscape occupied by humans from ∼14 to 7 ka.

2. Methods

The multi-proxy data sets from this study are evaluated in the context of a sequence stratigraphic framework to create a model of deposition in the landscape at Kabua Gorge through space and time. This study combines *in situ* field strata measurements, with new and published AMS radiocarbon dates (Beck, 2015; Beck et al., 2015; Wilson, 2016; Allen, 2017; Beyin et al., 2017), and data sets generated from samples collected from within measured sections.

2.1. AMS radiocarbon analysis

AMS radiocarbon dates were measured from the mollusc *Melanoides tuberculata*. Results were calendar calibrated using the IntCal13 database (Reimer et al., 2013) and included as calibrated years before present (cal BP) where present is defined as 1950 AD (Talma and Vogel, 1993). Two sigma calibrated ages are used when discussing the chronology. Results with multiple intercepts on the calibration curve have been averaged. No reservoir correction was applied based on the findings of Garcin et al. (2012) and Beck (2015) which showed negligible offset in AMS radiocarbon ages.

2.2. Stratigraphy/sedimentology

Fieldwork for this project was conducted over the course of 5 separate field seasons spanning 2011–2016. Eight stratigraphic sections were measured across the study area. Each unit was described in the field, including identifying all molluscs to the genus level, and discrete samples were collected for the subsequent analyses described below. Sections locations and elevations were recorded and confirmed over multiple field seasons using a hand-held GPS.

2.3. Stable isotope analysis of pedogenic carbonates

One paleosol forming on a black clay unit was identified in the study area. It was classified as paleo-Vertisol based on wedge ped structures and pedogenic slickensides (Fig. 2). The significance of this unit is elaborated upon in 3. Results and Interpretation and 4. Discussion. This paleosol was sampled at six localities (15, A, B, C, D, and KBA-07) (Fig. 1) with at least 15 individual pedogenic carbonate nodules collected from each locality. For localities A, B, and C, samples were collected *in situ* from at least 50 cm below the upper boundary of the paleosol to ensure that the soil carbonates formed in equilibrium with soil CO_2 (Cerling and Quade, 1993; Levin et al., 2011). For localities D, 15, and KBA-07, nodules were recovered from the surface as this was the only place they were found. During collection, nodules that formed around shells, which can affect the isotopic signature (e.g., Michel et al., 2013), or showed evidence of recrystallization were avoided.

In the lab, nodules were rinsed with deionized water to remove clay. Nodules were processed in two separate ways. For a subset of samples from KBA-07 whole nodules were powdered using a mortar and pestle so measurements on these samples integrated across the entire nodule from exterior to interior. These data points represent bulk analyses of the entire nodule. Samples from all other localities, including a second set of nodules from KBA-07, were broken open and drilled using a Dremel, following the methods of Levin et al. (2011). 120–160 μg of

Fig. 2. a) Black clay with pedogenic overprint from the Kabua black clay at KBP-15, Jacob staff for scale (1.6 m) and b) example of large soil ped showing characteristic pedogenic slickenslides.

sample material was loaded into the Hamilton Isotope Lab's Thermo Delta V CF-IRMS and Gasbench instrument and run bracketed by laboratory standards (LECO, NBS-18, CaCO3- Merk, NBS-19) and are reportd relative to the Vienna Pee Dee Belemnite (V-PDB) reference standard and presented in δ-values in ‰.

Data from the pedogenic carbonates was averaged across each nodule and each sample site. Adjusted values were then used to calculate percent woody cover following the equation of Cerling et al. (2011):

$$f_{WC} = \{\sin[-1.00688 - 0.08538 * (\delta^{13}C_{carbonate} - 140/00)]\}^{2}$$

As indicated above, a 14‰ offset was subtracted from the $\delta^{13}C$ values from the pedogenic carbonates ($\delta^{13}C_c$) following standard conversion to $\delta^{13}C$ of organic matter ($\delta^{13}C_{om}$) as outlined in Cerling (2014).

2.4. Diatom analysis

Samples analyzed came from two localities: shoreline proximal KSS and KLS ~1 km towards the modern lake (Fig. 1). At KSS, samples of sub-mm scale diatomaceous beds were taken opportunistically through a short, 2.4 m interval within the previously described lacustrine interval Phase 3 (Beck, 2015). Sampling at KLS targeted a unit characterized by interbedded sand and diatomaceous silt. These samples were associated with the AMS radiocarbon date 16-KLS-14.

Dry diatom sub-samples were weighed into glass scintillation vials and treated with 35% H_2O_2 at room temperature. Reactions were allowed to continue for 3 weeks, in order to digest organic material. Supernatant fluids were removed with an aspirator and samples were rinsed four times with reverse osmosis purified water. Known quantities of polystyrene microspheres were added to estimate diatom concentrations (Battarbee et al., 2001). Diatom extractions then were dried by evaporation onto number-1 type coverslips using small-3D printed settling chambers that were designed to reduce settling, drying, and edge effects and result in an even distribution of diatom frustules across the coverslip. Coverslips were then mounted onto microscope slides with Zrax, a permanent high-refractive index medium. Slides were analyzed at 1000× magnification with a transmitted light microscope (Leica DM2500) under Differential Interference Contrast optical illumination. Diatom frustules were identified to the most specific taxonomic level possible. When possible, at least 300 diatom valves were identified from each sample interval.

2.5. Loss-on-ignition

Loss-on-ignition was performed to quantify the total organic and total inorganic carbon content from seven sediment samples collected from an organic-rich, black clay outcropping around the study area. Samples were powdered with a mortar and pestle prior to analysis following a modification of the LacCore standard operating procedure (LacCore, 2013). Three heating steps of +8 h at 55 °C in a drying oven, 550 °C for 4 h, and 1000 °C for 2 h were used to determine percent water, total organic carbon (TOC), and total inorganic carbon (TIC) respectively. The analyses were performed in an Isotemp muffle furnace at Hamilton College.

3. Results and Interpretation

3.1. Chronology and stratigraphy

Three lake highstand events are recorded at Kabua Gorge, dated to 13,870 ± 120 cal BP (Phase 1), 13,040 ± 50 cal BP (Phase 2), and 11,740 ± 230 cal BP (Phase 3) (Beck, 2015; Beck et al., 2019). These lake phases were all lithologically similar, being characterized by deposition of laminated to thinly-bedded gray clay to silt. Isolated diatomaceous laminae occurred sporadically within the otherwise siliciclastic sequence. Fine to medium, quartz-dominated sands with ripple laminations, cross-beds, and mollusc lenses separated each phase (Beck, 2015). New AMS radiocarbon dates from the mollusc *Melanoides tuberculata* from this study have been added to those previously published by Beck et al. (2019), van der Lubbe et al. (2017) and Beyin et al. (2017) (Table 1). Together this compiled dataset allows for a more comprehensive look at the chronostratigraphic relationships and thus the evolution of the paleoenvironment of Kabua Gorge. The dates provided by this study of 8280 ± 85 cal BP (16-KLS-14) and 7350 ± 70 cal BP (15-KBA-07) are significantly younger than the Late Pleistocene Phases 1–3. Stratigraphically, sediments yielding younger ages are higher in the section than Phase 1–3 and thus we propose the addition of a lacustrine Phase 4 to the stratigraphic record of Kabua Gorge. Previously, these sediments, while described, were not integrated into the Holocene lacustrine record because without age control, they could not be connected to the broader context of lake level history. Phase 4 is lithologically distinct from Phases 1–3 as it is comprised exclusively of organic-rich, black clay. North of the Kalokol River, this black clay Phase 4 unit has been overprinted by pedogenesis so it displays a gradation of subsequent soil formation across a landscape. Phase 4 was previously interpreted as indicative of a reduced, marsh environment on the basis preliminary data indicating it contained pyrite, had a high total organic carbon content, and displayed pedogenic overprinting (Beck, 2015). These claims were reevaluated by integrating new stratigraphic sections to expand the spatial distribution of the study area with more robust geochemical data including expanded total organic carbon data and stable isotopes on pedogenic nodules collected from within Phase 4. Two transects through the study area, SW-NE and SE-NW, provide more details about the spatial variability of the paleoenvironment both parallel and perpendicular to the paleoshoreline.

Sections RR1, KMS, and KLS span a SW to NE transect from the shoreline moving basinward (Fig. 3). Lithologically, these sections were correlated on the basis of the Phase 4 black clay. The stratigraphy becomes more hetereogeneous in the basinward sections, likely due to increased accommodation space, and thus a sequence stratigraphic approach is necessary to reconstruct how these units were related in space and time. The distal part of the sequence records more subtle changes in the depositional regime that are contained within the cross-bedded sand units between lacustrine Phases 1, 2, and 3 in the shore-proximal sections. Thus, what is represented as a depositional hiatus (or sequence boundary) at the margin is recorded in the KMS and KLS sections. Another key difference in the record is age of the sediments in each section. AMS radiocarbon dates from molluscs associated with the black clay (Table 1) demonstrate that the lithology associated with Phase 4 is time transgressive. Out in the basin, sample 16-KLS-14 (8280 ± 85 BP) is at least 930 yrs older than the shoreline-proximal

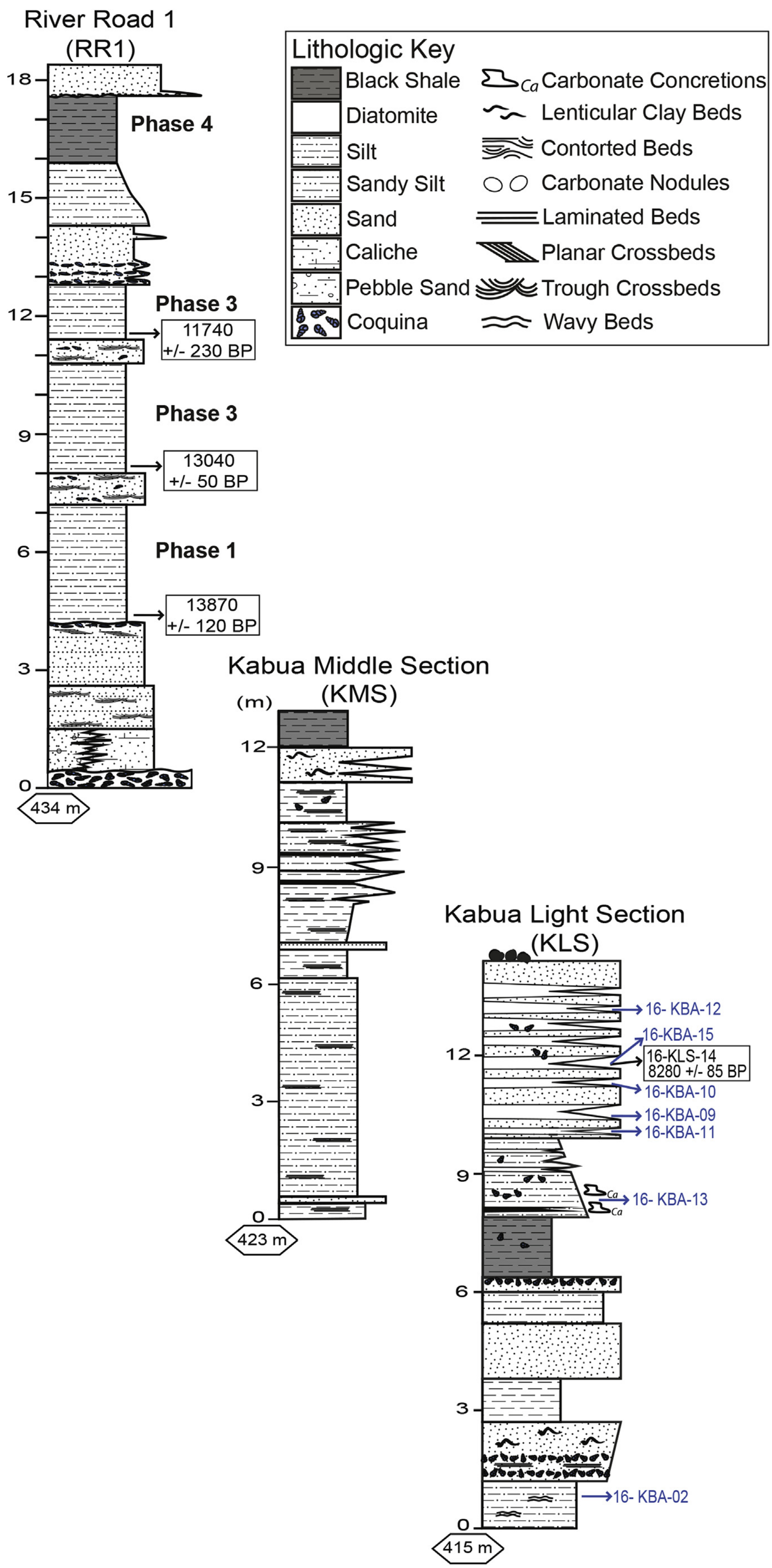

Fig. 3. Stratigraphic columns hung by elevation from RR1 to KLS (ie into the basin from west to east). Stratigraphic positions of radiocarbon ages indicated with black arrows and ages in boxes next to columns. Diatom samples are shown in stratigraphic position in blue.

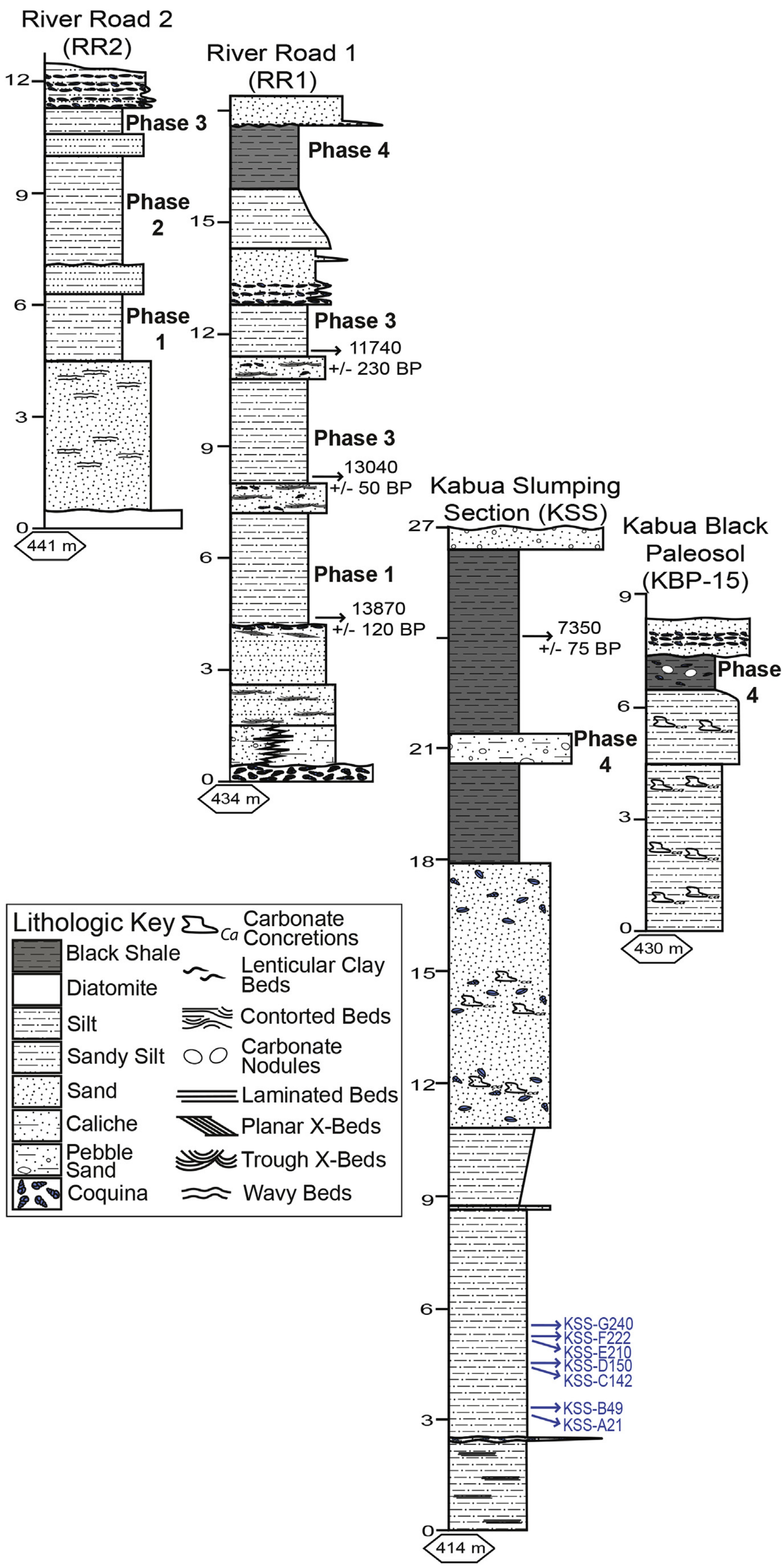

Fig. 4. Stratigraphic columns hung by elevation from RR2 to KBP (ie south to north parallel to the shoreline). The sampling localities KBP-A to KBP-D are the lateral equivalent of the upper 3 m of KBP-15. Stratigraphic positions of radiocarbon ages indicated with black arrows and ages in boxes next to columns. Diatom samples are shown in stratigraphic position in blue.

sample 15-KBA-07 (7350 ± 75 BP). This stratigraphic relationship complicates lithocorrelation solely based on the sedimentology of the units and highlights the dynamic nature of the system responsible for depositing them. AMS radiocarbon dates from the shoreline-proximal (RR1) and distal (KLS) sections show a significant offset in the age of the sedimentary record and support the sequence stratigraphic interpretation of these units.

Sections RR2, RR1, KSS and KBP represent a ~SE to NW transect, roughly paralleling the paleoshoreline (Fig. 4). Again, these sections are hung lithologically on the Phase 4 black clay. However, considerable variability in the thickness of the Phase 4 deposits and variable degrees of pedogenesis documented in the study area suggest a further degree of complexity in the depositional regime. Phase 4 was 1.7 m in the RR1 section but increased in thickness to 2.9 m at KBP ~2 km to the north. The thicker Phase 4 was also characterized by increased pedogenesis, unlike the previous Phases 1–3. South of the modern Kalokol River, the black clay was laminated and showed limited to no pedogenic overprinting. North of the Kalokol River morphological features of a paleo-Vertisol with horizonation, wedge peds, pedogenic slickenslides, and pedogenic carbonate nodules were identified in the sections (Fig. 2). However, this unit still contained evidence of sub-aqueous conditions as it contained molluscs such as the aquatic pulmonate *Pila ovata*, which prefers swampy conditions.

3.2. Pedogenic carbonates

All data from stable isotope analyses is presented in Table 2. Measurements of $\delta^{18}O$ ranged from −4.48 ± 0.056‰ to −0.25 ± 0.060‰. Due to significant uncertainty surrounding the sourcing of precipitation falling on the soil and the effects of temperature and evaporation during soil formation, $\delta^{18}O$ values are difficult to interpret and will not be further discussed, but are reported here for completion. For $\delta^{13}C$ measurements there was more variability, with values spanning 6.56‰, from −8.85 ± 0.072‰ to −2.29 ± 0.053‰. The $\delta^{18}O$ and $\delta^{13}C$ are presented in a cross plot (Fig. 5a) and a histogram of $\delta^{13}C$ color-coded by site (Fig. 5b). These isotopic ranges are interpreted to represent spatial variability in pedogenic carbonates, as opposed to temporal changes in paleoenvironment for two reasons. 1) Stratigraphically, these nodules came from the same paleosol and were all sampled > 50 cm below the upper contact of the black clay unit. 2) The process of pedogenesis is inherently a time-averaging one, as soils with pedogenic carbonate form on the order of hundreds to thousands of years (Targulian and Krasilnikov, 2007). Nodules forming in the soil represent that sum of the pedogenic processes acting on a soil over the entire period of pedogenesis, and therefore only reflect a snapshot of this stable landscape rather than any temporal trends regardless of depth in the soil profile. However, a histogram of $\delta^{13}C$ data from replicate samples at each locality highlights the variability between sites (Fig. 5b). Thus the proxies stemming from these data reflect paleovegetation variability across a relatively flat landscape utilized by humans as opposed to shifts in paleovegetation through time. The $\delta^{13}C$ data from pedogenic carbonates from each nodule was averaged for each individual sample locality (Table 2). These averages were then used to calculate percent woody cover (including a 95% confidence interval) using the equation outlined by Cerling et al. (2011). Using percent woody cover each sample site was categorized using the United Nations Educational, Scientific and Cultural Organization (UNESCO) classification of African vegetation (White, 1983) into one of five principal vegetation types: 1) forest, 2) woodland/brushland/thicket/shrubland, 3) wooded grassland, 4) grassland, and 5) desert. Because the samples in this study came from ~1 km^2 area, this allowed for a high-resolution paleolandscape reconstruction. Looking at a transect from north to south (moving from the margin of the Holocene depocenter towards the center of it which corresponds to the position of the modern Kalokol River), the percent woody cover varies across the study area from 26.9% in the north (16-KBA-09D) to 39.4–44.9% (16-KBA-09A-C) to 23.5% (16-KBA-15) and then finally 16.6% in the south (KBA-07). When converted to percent woody cover, the conventional interpretation would be a transition from wooded grassland at KBP-D to woodland/brushland/thicket/shrubland at KBP-A, B, and C, before transitioning back to the more open wooded grassland environment at KBP-15 and KBA-07. These data demonstrate the high degree of spatial variability in terms of vegetation over the study area.

One additional finding was that the method of nodule sample preparation (whole nodule versus drilled subsamples) had no significant impact on the stable isotope measurement. For KBA-07 where both methods of analysis were performed, the mean $\delta^{18}O$ and $\delta^{13}C$ of the bulk whole nodules were −3.23 ± 0.06‰ and −3.38 ± 0.05‰ respectively while for the drilled nodules, the means were −3.22 ± 0.04‰ and −3.46 ± 0.03‰ (Fig. 5). The difference between the means of the two types of samples was 0.01‰ for $\delta^{18}O$ and 0.08‰ for $\delta^{13}C$. This indicates that the nodules were homogeneous in composition.

3.3. Diatom analysis

The diatom data from this study provides additional information about lacustrine conditions in different positions relative to the shoreline through time. This is significant from a resource perspective as humans were leveraging both terrestrial and aquatic resources (including availability of fresh water) in this location. Therefore, it is essential to integrate paleolimnological data into the landscape perspective. Overall, diatom assemblages are characterized by freshwater taxa. This is indicated both by the diatom assemblages and the pristine preservation of the individual valves and long, delicate chains, particularly within KSS. There are some noteworthy differences between the sites that indicate a change in the overall conditions of the lake through time (Fig. 6). The diatom assemblages from the mm-scale beds at KSS are all similar in composition, being dominated by *Aulacoseira*. This indicates a fresh, well-mixed lake, potentially with slightly elevated phosphorus and silica levels (Kilham, 1990; Owen and Utha-aroon, 1999; Stone et al., 2011). However, the presence, despite their relatively low abundance, of *Stephanodiscus* points to times when the silica concentrations were more limited (Haberyan and Hecky, 1987; Scholz et al., 2003). This seemingly contradictory evidence is interpreted to reflect seasonal variability in nutrient availability, likely in response to increase local runoff during biannual monsoons. The lack of substantial periphytic taxa in these intervals, and the high diatom concentration in the sediments, suggests that the lake was probably fairly deep at the depocenter and highly productive.

Despite its more basinward sampling position relative to the modern lake, samples of diatomite from the younger KLS record a shallower lacustrine environment than those sampled from the older, more shore proximal KSS site within the KSS. The assemblages from KLS were dominated by tychoplanktonic and periphytic diatoms, with the exception of one sample near the base of the section (KLS-13). While the assemblage at KLS-13, like the KSS samples, was dominated by *Aulacoseira*, the ringleistes were typically the only part of the diatom frustules preserved in this sample. This finding is significant because the ringleistes, particularly from the genera *Aulacoseira*, are elements of robust silica in the skeleton and thus are likely the last to disappear as frustules are dissolved under increased alkalinity in the lake (Ryves et al., 2009). They could also be concentrated through mechanical reworking of older, *Aulacoseira*-rich lacustrine sediments from further down in the section. Therefore, the skew towards *Aulacoseira* in the KLS-13 assemblage is likely taphonomical and less robust diatoms, such as *Nitzschia,* while potentially present in the lake at this time, were not well preserved in the sedimentary record. Since the majority of the lacustrine facies at Kabua contain at least some diatomaceous component, the difference in the KLS-13 assemblage relative to the rest of this section is likely a signal of more alkaline water chemistry. The rest of

Table 2
Pedogenic carbonate data with woody cover interpretation. The * denotes samples where the whole nodule was powdered and analyzed, yielding an integrated isotopic value.

Locality	Sample ID	δ13C (‰)	δ13C-StDev	δ18O (‰)	δ18O-StDev	% Woody Cover
KBP-15	16-KBA-15-01	−3.09	0.034	−2.83	0.056	**23.50%**
KBP-15	16-KBA-15-02	−3.61	0.029	−3.17	0.057	
KBP-15	16-KBA-15-03	−4.9	0.049	−1.93	0.052	
KBP-15	16-KBA-15-04	−5.08	0.035	−2.05	0.049	
KBP-15	16-KBA-15-05	−4.88	0.047	−2.65	0.057	
KBP-15	16-KBA-15-06	−4.79	0.029	−2.61	0.055	
KBP-15	**AVERAGE**	**−4.39**	**0.037**	**−2.54**	**0.054**	
KBP-A	16-KBA-09A-01	−5.4	0.023	−1.78	0.035	**39.40%**
KBP-A	16-KBA-09A-02	−5.91	0.037	−0.92	0.068	
KBP-A	16-KBA-09A-03	−5.22	0.031	−1.57	0.038	
KBP-A	16-KBA-09A-04	−7.17	0.028	−1.05	0.034	
KBP-A	16-KBA-09A-05	−6.4	0.048	−1.05	0.041	
KBP-A	16-KBA-09A-06	−7.34	0.049	−3.35	0.051	
KBP-A	16-KBA-09A-07	−6.93	0.047	−3.48	0.074	
KBP-A	16-KBA-09A-E01	−8.85	0.072	−0.46	0.074	
KBP-A	16-KBA-09A-E02	−4.51	0.14	−2.9	0.137	
KBP-A	**AVERAGE**	**−6.41**	**0.053**	**−1.84**	**0.061**	
KBP-B	16-KBA-09B-01	−6.16	0.036	−2.86	0.036	**42.40%**
KBP-B	16-KBA-09B-02	−5.76	0.042	−2.92	0.042	
KBP-B	16-KBA-09B-03	−6.51	0.042	−3.07	0.042	
KBP-B	16-KBA-09B-04	−6.37	0.038	−2.98	0.038	
KBP-B	16-KBA-09B-05	−8.28	0.052	−4.48	0.052	
KBP-B	16-KBA-09B-06	−7.7	0.06	−3.09	0.06	
KBP-B	**AVERAGE**	**−6.8**	**0.045**	**−3.23**	**0.045**	
KBP-C	16-KBA-09C-01	−7.95	0.014	−1.12	0.033	**44.90%**
KBP-C	16-KBA-09C-02	−7.68	0.044	−1.35	0.053	
KBP-C	16-KBA-09C-03	−7.73	0.024	−1.51	0.036	
KBP-C	16-KBA-09C-04	−4.81	0.049	−1.77	0.059	
KBP-C	16-KBA-09C-05	−4.25	0.067	−1.86	0.025	
KBP-C	16-KBA-09C-06	−7.39	0.038	−0.93	0.038	
KBP-C	16-KBA-09C-07	−7.99	0.046	−1.38	0.053	
KBP-C	16-KBA-09C-E03	−8.7	0.05	−1.35	0.056	
KBP-C	**AVERAGE**	**−7.06**	**0.041**	**−1.41**	**0.044**	
KBP-D	16-KBA-09D-02	−5.36	0.016	−0.49	0.053	**26.90%**
KBP-D	16-KBA-09D-03	−6.1	0.053	−1.8	0.061	
KBP-D	16-KBA-09D-04	−4.94	0.06	−0.54	0.052	
KBP-D	16-KBA-09D-05	−6.15	0.051	−1.67	0.041	
KBP-D	16-KBA-09D-06	−6.4	0.019	−1.9	0.061	
KBP-D	16-KBA-09D-07	−4.92	0.039	−0.25	0.06	
KBP-D	16-KBA-09D-08	−5.05	0.057	−1.63	0.048	
KBP-D	16-KBA-09D-09	−4.27	0.052	−0.74	0.061	
KBP-D	16-KBA-09D-10	−4.42	0.061	−0.56	0.052	
KBP-D	16-KBA-09D-11	−2.67	0.05	−1.17	0.056	
KBP-D	16-KBA-09D-12	−2.43	0.055	−0.95	0.055	
KBP-D	16-KBA-09D-E04	−5.09	0.049	−0.49	0.048	
KBP-D	**AVERAGE**	**−4.82**	**0.047**	**−1.02**	**0.054**	

(*continued on next page*)

Table 2 (*continued*)

Locality	Sample ID	δ13C (‰)	δ13C-StDev	δ18O (‰)	δ18O-StDev	% Woody Cover
KBA-07	15-KBA-07A-D01	−3.94	0.034	−3.11	0.034	**16.60%**
KBA-07	15-KBA-07A-D02	−2.79	0.06	−3.6	0.041	
KBA-07	15-KBA-07A-D03	−2.91	0.039	−3.64	0.07	
KBA-07	15-KBA-07A-D04	−4.08	0.03	−3.29	0.068	
KBA-07	15-KBA-07A-D05	−3.56	0.046	−2.66	0.068	
KBA-07	15-KBA-07A-D06	−3.22	0.065	−3.32	0.071	
KBA-07	15-KBA-07A-D07	−3.91	0.064	−3.65	0.091	
KBA-07	15-KBA-07A-D08	−3.46	0.03	−3.06	0.051	
KBA-07	15-KBA-07A-D09	−3.21	0.053	−2.91	0.054	
KBA-07	15-KBA-07A-D10	−3.09	0.03	−2.98	0.034	
KBA-07*	1	−3.52	0.045	−3.18	0.065	
KBA-07*	2	−3.24	0.05	−3.33	0.071	
KBA-07*	3	−4.67	0.041	−2.91	0.063	
KBA-07*	4	−4.49	0.052	−2.99	0.067	
KBA-07*	5	−3.03	0.039	−3.76	0.03	
KBA-07*	6	−2.54	0.051	−4.06	0.055	
KBA-07*	7	−2.29	0.053	−3.63	0.079	
KBA-07*	8	−2.95	0.064	−3.28	0.069	
KBA-07*	9	−3.75	0.076	−3.27	0.088	
KBA-07*	10	−4.39	0.037	−2.98	0.042	
KBA-07*	11	−2.87	0.058	−3.24	0.074	
KBA-07*	12	−4.3	0.073	−3.29	0.092	
KBA-07*	13	−2.78	0.071	−3.76	0.087	
KBA-07*	14	−2.72	0.032	−3.45	0.029	
KBA-07*	15	−3.26	0.032	−3.39	0.047	
KBA-07*	16	−3.94	0.029	−1.55	0.041	
KBA-07*	17	−2.96	0.03	−2.88	0.042	
KBA-07*	18	−3.69	0.03	−3.5	0.04	
KBA-07*	19	−3.18	0.035	−3.34	0.063	
KBA-07*	20	−2.74	0.038	−3.8	0.037	
KBA-07	**AVERAGE**	**−3.38**	**0.046**	**−3.26**	**0.059**	
Average		**−4.87**	**0.049**	**−2.4**	**0.06**	
Range		**6.56**	**-**	**−4.73**	**-**	

the assemblage at KLS, however, is dominated by *Nitzschia*. This indicates lake conditions that are fresher than those from KLS-13 (as the more delicate genus is preserved) but more alkaline than the KSS samples.

3.4. Total organic carbon

The percent carbon values presented in Table 3 are relative to the dry weight of each sample. The total organic carbon (TOC) is the focus of this analysis as it reflects aspects of the carbon cycle in the Kabua depositional environment. Sample 16-KLS-07, collected from the homogeneous black clay unit in section KLS has the highest TOC (9.41%). However, all of these samples have a TOC > 2% and are thus, by definition, sapropels. Thus, in this paleoenvironment carbon burial and preservation was high.

4. Discussion

Reconstructing the landscape at Kabua Gorge is essential for understanding the distribution of resources available to anatomically modern humans inhabiting this region. To this end, the data presented in this study is analyzed within a stratigraphic context and paleovegetation is reconstructed using both the amount of TOC and, on the finer scale of resolution, stable isotope results from pedogenic carbonates. The combinations of proxies presented here allows for reconstruction of lacustrine conditions (sedimentology and diatom record) to terrestrial ones (TOC and pedogenic carbonates) to provide a more holistic interpretation of the aquatic and subaqueous paleoenvironment that humans encountered through the AHP.

4.1. Stratigraphic interpretation

The composite stratigraphy at Kabua Gorge is comprised of at least four phases of lacustrine highstand that allow for further refinement of existing lake-level curves through the AHP (Fig. 7). Evaluating the stratigraphic information within the context of Holocene lake-level curves (Garcin et al., 2012) demonstrates that the black clay unit of lacustrine Phase 4 was likely deposited during rapid changes (both regression and transgression) where the shoreline was moving across the landscapes and shifting this marginal lacustrine marsh facies along with it. This spatial and temporal relationship is highlighted through comparison between the basinward KLS section to the shoreline-proximal KSS section as both sections include radiocarbon dates (Fig. 8). It necessitates a sequence stratigraphic interpretation of the depositional units in the study area.

There are strong lithologic and biological indicators that Phase 4 sediments across Kabua Gorge represent restricted water conditions in a fluctuating marsh-like environment. The first line of evidence is high TOC, which indicates deposition in a reducing environment (Vigliotti et al., 2011; Hilgen, 1991). One way to produce that type of low-oxygen setting is through a deep, stratified lake. However, modern lake Turkana is well-mixed due to a combination of its relatively shallow depth and the pervasive wind action by the Turkana Jet (Nicholson, 1996) which drives the currents that stir the lake (Yuretich, 1979). As evidenced by the diatom assemblages observed in the KSS diatomites, Holocene Lake Turkana was likely also subjected to pervasive wind-driven mixing which might have had significant impacts on aquatic ecosystems as proposed by Ashley et al. (2017). If thermal or chemical stratification were to develop, the lake would need to be much deeper than it is today, and would have a distinctly different diatom flora present (Stone et al., 2011). The diatom record also supports the relative shallowing of the lake through time as the accommodation space filled with sediment. Samples from the older, diatomaceous partings in KSS represent an open freshwater assemblage and exhibit pristine preservation, pointing to a lake that was significantly less alkaline than the modern during Phase 3. Comparatively, the diatoms from KLS,

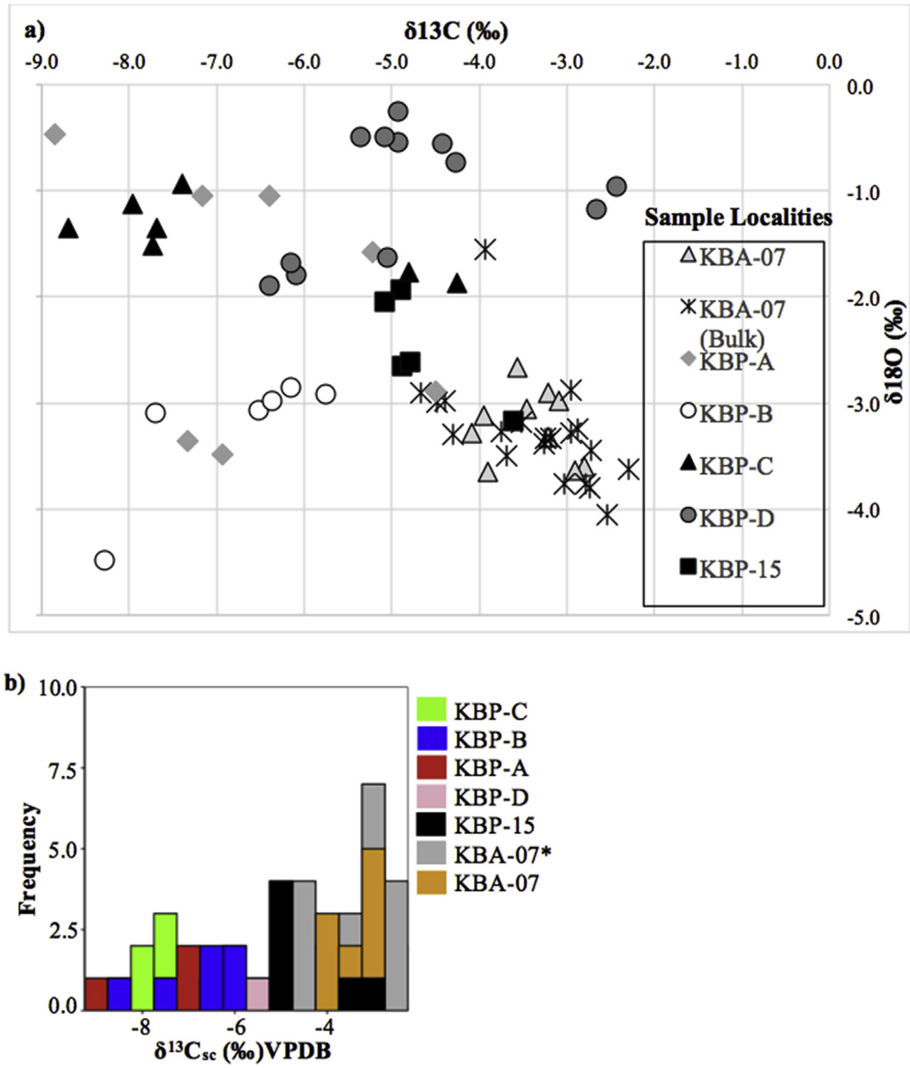

Fig. 5. a) Cross plot of $\delta^{13}C$ and $\delta^{18}O$ data from individual soil carbonate nodules from each site. KBA-07 (bulk) samples are data from whole nodules which were powdered and then analyzed. These data demonstrate that there was no systematic offset between bulk samples and drilled samples, indicating the homogeneity of the pedogenic carbonate. b) Frequency plot of all isotopic data binned in 1 per mille increments and color coded by site. Sites KBA-07 and KBP-15 are dominated by C_4 vegetation while the other sites appear more mixed.

which represents a time-synchronous, lateral facies transition from the Phase 4 black clays of the KBP section, is characterized by a more benthic assemblage of diatoms and a slightly more alkaline lake environment. These lines of evidence suggest that water depth at Kabua was shallower than during the deposition of the earlier Phases 1–3. The black clay unit is located at a maximum elevation of 452 m (RR1 section), which is 92 m above the elevation of the modern lake (~360 m asl (Garcin et al., 2012)). The elevation of the spillway from Lake Turkana into the White Nile is at 455–460 m asl. While sub-basins of the Turkana Basin, such as the volcanically active South Basin, are tectonically active during the Holocene (Melnick et al., 2012), the majority of the system has been tectonically quiescent since 200,000 BP (Feibel, 2011). Assuming tectonic stability, the maximum possible water depth at Kabua Gorge for the black clays would only be 3–8 m as once the spillway elevation was breached, the lake could not get deeper than this level. Even in overflow conditions, the region around Kabua Gorge would have been shallow, making stratification, including prolonged establishment of a localized chemocline, unlikely. A more likely scenario is that the black clays were deposited in a fringing marsh or lagoonal type setting.

This hypothesis is further supported by the presence of pedogenic carbonate nodules dispersed throughout the black clay that indicate the area was subaerially exposed and soil formation occurred. Nodule formation may have occurred during multiple hiatuses in black clay deposition (though the lack of multiple horizons of pedogenic carbonates makes this unlikely) or at some time following the deposition of the unit. Either way it also refutes the interpretation that the black clays of Phase 4 were deposited in a deep lake environment. Walther's Law states that conformable facies must have been laterally adjacent and therefore supports the model of fringing marsh being abandoned and overprinted by soil processes as lake level fell. Finally, biological evidence comes in the form of the swamp pulmonate, *Pila ovata*, that are found mixed in with lacustrine molluscs (*M. tuberculata*, *M. nilotica*, *C. consobrina*, *Etheria elliptica*). This assemblage suggests that Kabua Gorge was a dynamic, fluctuating margin that was sometimes exhumed and sometimes inundated, potentially on a seasonal basis during the time when this unit was deposited. Stratigraphic interpretation in the Kabua Gorge study area is complicated by the dynamic lake level history as during lowstands, the Kalokol River incised through the lacustrine sediments, creating irregular topography that then later was infilled with subsequent lacustrine deposits. Using radiocarbon dating and a sequence stratigraphic framework, this study demonstrates the spatial complexity surrounding the deposition of the Phase 4 black clays within this fluctuating lake marine. This interpretation is similar to what

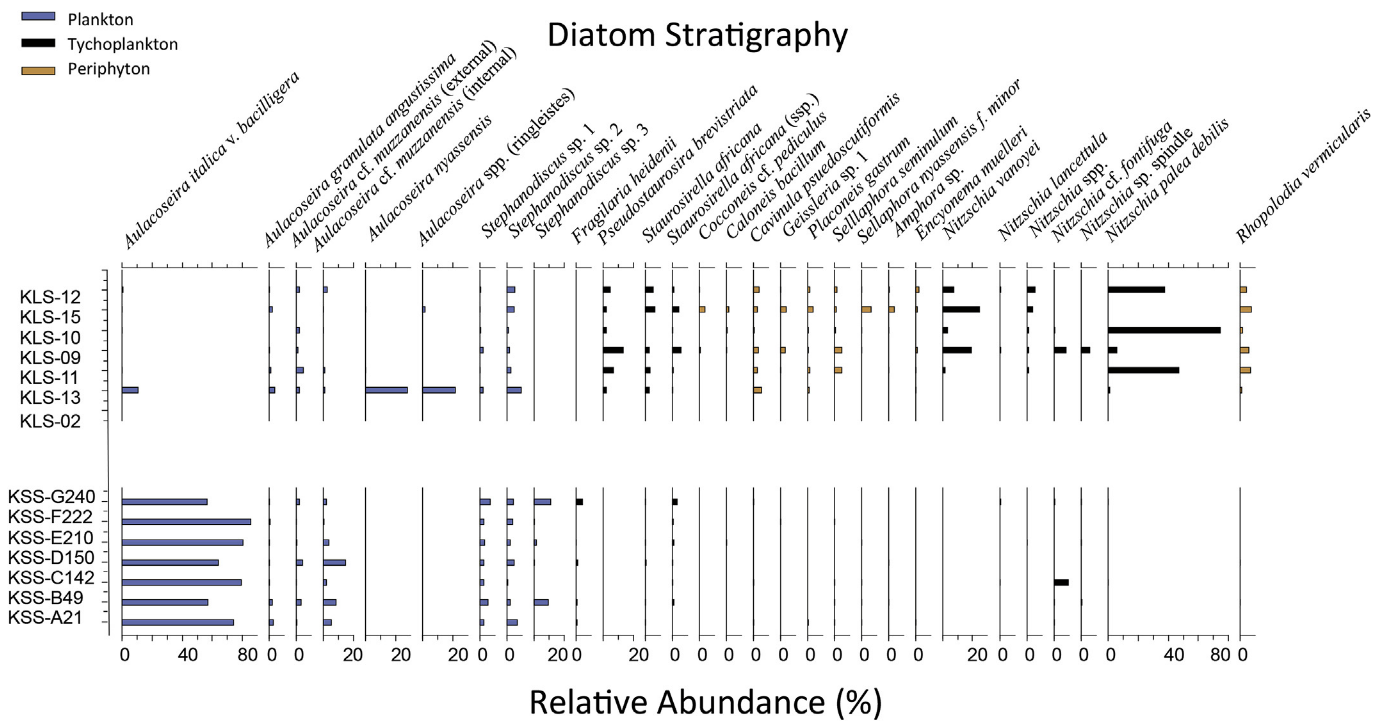

Fig. 6. Plot of diatom assemblages from high-resolution sampled intervals within two sections that are presented in relative stratigraphic order with the older section KSS at the bottom and the younger KLS samples on top. Diatoms are color coded by functional groups based on where they likely were in the water column.

Table 3
Loss on ignition TOC results from black clays from across the study area.

Sample ID	Section	% TOC	% TIC
15-KBA-08	RR2	5.55	1.69
12-Kabua-35	RR1	4.93	1.59
12-Kabua 22a	RR1	3.97	3.84
15-KBA-07b	KSS	6.72	1.36
16-KLS-07	KLS	9.41	1.07
16-KLS-16	KLS	6.75	1.87
16-KBP-07	KBP	6.97	1.59

occurs in the modern system, where meters of lake level change can expose kilometers of shoreline. However, the increase in local precipitation and fresher lake water during the AHP create a highly productive environment that supported more diverse vegetation, including a freshwater marsh.

4.2. Paleoenvironmental reconstruction

The high TOC preserved at Kabua is relatively unique to the Galana Boi Formation in the Turkana Basin. A "black shale facies" was included in the original formation designation and was interpreted to represent an anoxic, restricted lagoonal environment (Owen and Renaut, 1986). However, on the East Side of the basin where this description was made, this unit was limited to a maximum thickness of 4 cm to 1 m. In Kabua, this facies becomes volumetrically more significant and even warrants the designation as a distinct lacustrine Phase 4 for the record. Unlike Phases 1–3, Phase 4 is recording a marginal marsh environment, rather than a conventional highstand. The presence of pedogenic overprinting (paleosol formation) indicates that this horizon was a paleocatena (series of coevolving soils forming across topography with similar parent material and climate (Klaus et al., 2005)) located on the margin of Lake Turkana. From a resource availability perspective, this paleocatena is far more significant for humans than a littoral lacustrine deposit would be because the marsh would be a direct source of sustenance both in terms of foraging/fishing opportunities in shallow water and access to fresh drinking water.

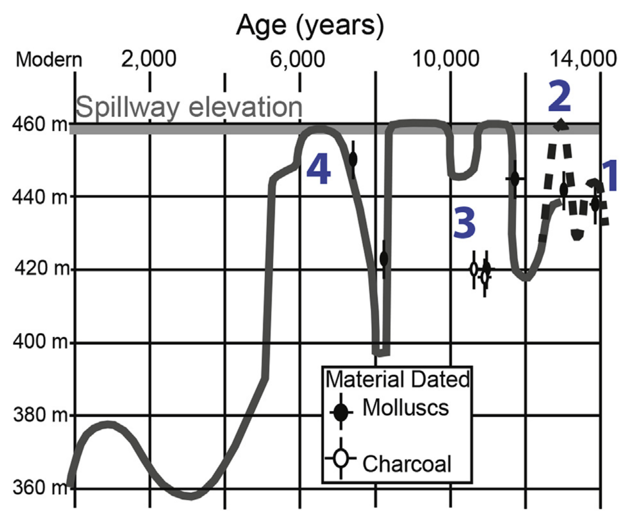

Fig. 7. Reconstruction of lake levels in the Turkana Basin during the AHP based on Garcin et al. (2012) and extended back to ~14,000 yrs with dashed lines as lake levels are not tightly constrained from the sedimentary sequence at Kabua Gorge alone (see Beck et al. (2019) for full discussion). The two youngest dates are associated with black clay deposits and strongly suggest that these units are closely associated with the shoreline of Holocene Lake Turkana. These data plot on a regressive and transgressive phase and thus support the hypothesis that the corresponding black clay units are time-transgressive reflecting the position of the littoral margin of the lake.

Interestingly, despite the clear reducing signal of the black clay, at Kabua, this unit was clearly overprinted by a paleo-Vertisol as evidenced by observations of vertic features such as wedge peds and pedogenic slickensides. Vertisols form in environments with seasonal wetting and drying of smectitic clays which must dry out for a period long enough for deep desiccation cracks to form (Nordt and Driese, 2009). Therefore, while marshy, lagoonal conditions dominated the

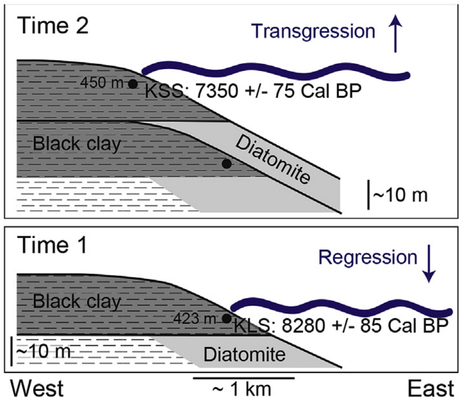

Fig. 8. Schematic model of time-transgressive relationship responsible for the deposition of the black clay. During Time 1, the lakeshore was at an elevations of ~420–425 m during a regressive phase according to Fig. 7. This is in agreement with the elevation of 423 m for the dated sample from KLS. The lake continued to drop rapidly down below 400 m before a transgressed occurred. By Time 2, the lake level was up to ~450 m and more black clay was deposited (as recorded at KSS) and pedogenically overprinted during subsequent periods of exposure. This model visually explains how the lithologically similar black clay units are actually not synchronous in their deposition.

deposition of this unit, the study area also experienced repeated subaerial exposure and desiccation. The data support the interpretation that, rather than one long depositional hiatus, pedogenic overprinting on the Phase 4 black clays occurred during repeated short periods of exposure over millennia that were short enough in duration that erosion between wet/dry cycles was minimal. These cycles could have operated on a scale of annual cyclicity driven by monsoons or intra-annual variability in response to events such as El Niño-Southern Oscillation.

Returning to the interpretation of the paleovegetation as a function of percent woody cover, the conventional model of C_4 vegetation being limited to arid adapted grasses and C_3 plants represented woody vegetation, herbs, and forbs contradicts the data about the broader depositional framework of the study area. The model at Kabua of a transect moving from open to closed before becoming more open again in the paleo-depocenter is not supported by the sedimentological evidence. Based on the local topography, we would anticipate that conditions would become wetter, as opposed to drier, moving southward along this transect. An alternative interpretation of this data is that the increase in C_4 vegetation is actually due to the presence of C_4 wetland plants, including wetland adapted grasses and sedges such as papyrus (Jones, 1988) (Fig. 9). Factors such as abundance of nitrogen and especially phosphorus might also favor the growth of certain wetland-adapted C_4 vegetation over C_3 (Mantlana et al., 2008). In the wetland C_4 model, the north-south transect would actually represent an increase in moisture moving from the margin of the study area into the depocenter, which is much more in line with a broad interpretation of the structural and sedimentological configuration of the study area. This interpretation highlights the importance of integrating proxy records holistically into their stratigraphic context. We strongly advocate for further study of the contribution of C_4 wetland vegetation on the development of pedogenic carbonates in modern environments to better quantify their contributions to the paleorecord. The record at Kabua demonstrates the high degree of landscape variability in a marginal lacustrine environment. The pedogenic carbonate samples used in this study came from an area less than 1 km in length and 0.3 km wide. This > 20% change in the amount of woody cover across the area might point to localize woody vegetation similar to the modern riparian woodlands fringing modern rivers in the Turkana Basin. From a human perspective, this means that populations had easy access to resources from a range of sub-environments from wooded grasslands to bushlands to marshes.

4.3. Resource availability

Human occupation on lakeshores has been underestimated in the archaeological record due to the transient nature of these sites as they shift in response to changes in lake level (Stewart, 1991). However, at Kabua Gorge, the low energy marsh recorded during Phase 4 of the record provides an important window into the paleoenvironment and thus the resources available to populations living in this area during the AHP. One essential requirement for survival is fresh drinking water without which animals, including humans, cannot survive more a few days (Cuthbert et al., 2017; Popkin et al., 2010). The enhanced moisture during the AHP resulted in increased availability of potable water in the Turkana Basin, as what today are ephemeral streams would have flowed more frequently (potentially even perennially) and the opening of Lake Turkana into the Nile drainage freshened the system. The diatom record from this study demonstrates that the lake was deep and productive during the time of deposition for Phase 4 sediments in sections KBP-A-D, KBP-15, and KBA-07. This productivity provides the basis for the food chain supporting aquatic ecosystems. The swampy littoral zone at Kabua specifically provided access to key aquatic resources utilized by humans as evidenced by the archaeological and archaeofaunal records (Beyin et al., 2017; Prendergast and Beyin, 2018). This included fish, turtles, hippopotamus, and potentially shellfish (Prendergast and Lane, 2010; Prendergast and Beyin, 2018). Globally, the opportunities provided by coastal resources such as access to shellfish are considered from a marine perspective (Bicho et al., 2011). In South Africa, the high density and predictability of shellfish beds has been proposed as a driver of cultural evolution towards co-operative societies stemming from the need to protect these valuable resources from outsiders (Marean, 2011). Lake Turkana during the AHP can be considered as an analog for these types of coast resources due to the presence of a lake since at least 14 ka (Beck et al., 2019), the large surface area of the water body, and the abundant mollusc and fish fossils. Extending this analogy to the cultural implications for human populations provides important paleoenvironmental context to the evidence of early warfare documented at the site of Nataruk ~90 km to the south of Kabua (Prendergast and Beyin, 2018; Mirazon Lahr et al., 2016). The productivity of the study area and its association with archaeological sites spanning from the Late Pleistocene to Middle Holocene suggests that this marsh paleoenvironment was resource-rich and thus a desirable place to occupy.

5. Conclusions

The region of Kabua Gorge was characterized by a resource-rich lacustrine margin that includes beach facies as well as organic-rich lagoonal or marsh facies. Marsh environments are interpreted from a black clay, Phase 4 unit on the basis multiple lines of evidence: 1) paleo-depocenter configuration, 2) high TOC of sediments, 3) mixtures of aquatic and terrestrial invertebrate fauna, 4) dominance of benthic diatoms distinct from plankton-dominated assemblages occurring in a prior highstand, and 5) sedimentological and geochemical properties of paleo-Vertisols and the pedogenic carbonates they contain. Interpretation of the stable isotope record is complicated by the potential abundance of wetland C_4 plants such as papyrus but through combining the sedimentology and proxy data, a more holistic reconstruction is possible. The paleoenvironment during the AHP, with percent woody cover of nearly 45% is very different from the modern, semi-arid and sparsely vegetated landscape (~10% woody cover) of today. The Kabua Gorge study area is unique because it presents the opportunity to tightly tie the archaeological record to the geological one. Dates published from the archaeological sites of Kokito and Dilit put the time of occupation for this area into the window when the lake was high and fresh (Table 1) (Prendergast and Beyin, 2018; Beyin et al.,

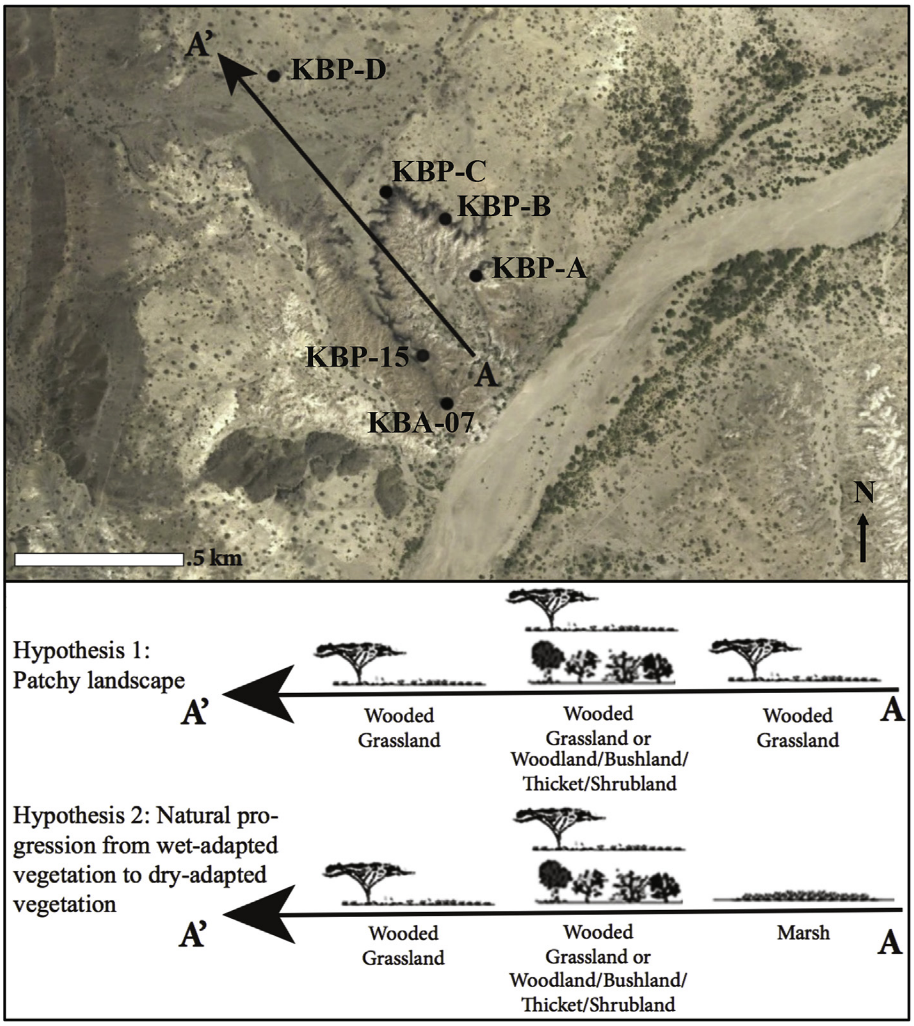

Fig. 9. Two possible interpretation of woody cover based on the stable isotope analysis of pedogenic carbonate nodules. The position of the transect A′ to A is shown on Fig. 1. In Hypothesis 1, the conventional interpretation of the $\delta^{13}C$ data from the pedogenic carbonates could be interpreted as a transition from the more open wooded grassland in the north of the study area to more closed environment in the center before becoming again more open on the south end of this transect. However, we favor Hypothesis 2, which interprets that higher percentage of C_4 vegetation in the south as this model fits with the broader depositional framework of the study area.

2017). At the onset of the AHP, there would have been abundant accommodation space at Kabua Gorge, as the area had likely been experiencing net erosion throughout much of the Middle to Late Pleistocene. Thus when the lake level rose at the onset of the AHP, it penetrated westward, into the gorge cut by the Kalokol River, flooding the area to the west of the ridge of Miocene Kalokol basalts. Humans appear to be tracking these changes, processing resources at the edge of the lake where it is most protected from high-energy wave action, in this case because of the basalt ridge. Through time, and due to the relative tectonic quiescence in this area, the accommodation space filled and the geologic record suggests that the resource-rich lake margin shifted basinward during Phase 4. We would anticipate that sites from this time period to be located eastward of the basalt ridge, closer to the modern basin. The later paleoenvironment provided abundant opportunities for resource acquisition for humans living in the area during the AHP. Identification of black clays could potentially aid in pinpointing areas with high potential for yielding archaeological sites because they indicate a highly productive paleoenvironment.

Author contributions

Authors CB, MA, CF, and EB collaborated on the fieldwork for this project. CB coordinated the research and lead the manuscript preparation, submission, and revision. MA lead the analysis of the data as part of her senior thesis project at Hamilton College. CF contributed intellectually to the development of the project and the fieldwork. EB contributed to the analysis of the pedogenic carbonate data. JS conducted the diatom analysis and interpretation. BW supervised the stable isotope data collection. CW collected pedogenic carbonate data from Kabua-07* and analyzed data in senior thesis project at Hamilton College. All authors provided input to the manuscript preparation and revision.

Conflicts of interest

The authors declare that the research was conducted in the absence of any commercial or financial relationships that could be construed as a potential conflict of interest.

Acknowledgements

For assistance in the field, we acknowledge the contributions for Francis Ekai (Turkana Basin Institute), Dominic Ikai (Nariokotome), and Mary Langworthy (Hamilton College). Lab support was provided by Alison Kingston (Hamilton College Isotope Lab student technician), and Joseph Mohan and Helena Bierly (Indiana State University Paleolimnology Laboratory). Funding from Hamilton College Dean of Faculty supported the 2016 fieldwork and the Hamilton College Donald Potter Award supported student participation for fieldwork. Additional support was provided by a Rutgers University Graduate School Special Study Award, Geological Society of America Student Research Grant, and AAPG David Worthing Family Grant.

Appendix A. Supplementary data

Supplementary data to this article can be found online at https://doi.org/10.1016/j.jafrearsci.2019.03.007.

References

Allen, M.M., 2017. Paleoenvironmental Reconstruction of the Holocene Galana Boi Formation at Kabua Gorge, Turkana Basin. Kenya [B.A.], Hamilton College.
Ashley, G.M., Ndiema, E.K., Spencer, J.Q.G., Harris, J.W.K., Kiura, P.W., 2011. Paleoenvironmental context of archaeological sites, implications for subsistence strategies under Holocene climate change, northern Kenya. Geoarchaeology 26 (6), 809–837.
Ashley, G.M., Ndiema, E.K., Spencer, J.Q.G., Harris, J.W.K., Kiura, P.W., Dibble, L., Du, A., Lordan, P.T., 2017. Paleoenvironmental reconstruction of Dongodien, lake Turkana, Kenya and OSL dating of site occupation during late Holocene climate change. Afr. Archaeol. Rev. 34, 345–362.
Barthelme, J.W., 1977. Holocene sites north-east of Lake Turkana: a preliminary report. Azania 12 (1).
Barthelme, J.W., 1985. Fisher-Hunters and Neolithic Pastoralists in East Turkana, Kenya.
Battarbee, R., Jones, V., Flower, R., Cameron, N., Bennion, H., Carvalho, L., 2001. Diatoms. In: Smol, J., Birks, H., Last, W. (Eds.), Tracking Environmental Change Using Lake Sediments, Volume 3: Terrestrial, Algal, and Siliceous Indicators. Kluwer Academic Publishers, Dordrecht, The Netherlands, pp. 155–202.
Beck, C.C., 2015. A Multiproxy Approach to Deciphering Terrestrial Climate Records from the Turkana Basin. Rutgers University, Kenya [Ph.D.].
Beck, C.C., Feibel, C.S., Wright, J.D., Mortlock, R.A., 2019. Onset of the African humid period by 13.9 kyr BP at Kabua Gorge, Turkana Basin, Kenya. Holocene p.0959683619831415.
Beck, C.C., Feibel, C.S., Beyin, A., 2015. In: Living in a Swampy Paradise: Associations between Archaeology and Marches from the African Humid Period. vol 47. Geological Society of America Abstracts with Programs, West Turkana, Kenya, pp. 441 No. 7.
Beyin, A., 2011. Recent archaeological survey and excavation around the greater Kalokol area, west side of Lake Turkana: preliminary findings. Nyame Akuma 75, 40–50.
Beyin, A., Prendergast, M.E., Grillo, K.M., Wang, H., 2017. New radiocarbon dates for terminal Pleistocene and early Holocene settlements in West Turkana, northern Kenya. Quat. Sci. Rev. 168, 208–215.
Bicho, N.F., Haws, J.A., Davis, L.G., 2011. Trekking the Shore: Changing Coastlines and the Antiquity of Coastal Settlement. Springer Science & Business Media.
Bloszies, C., Forman, S.L., Wright, D.K., 2015. Water level history for lake Turkana, Kenya in the past 15,000 years and a variable transition from the African Humid Period to Holocene aridity. Glob. Planet. Chang. 132, 64–76.
Boschetto, H.B., Brown, F.H., McDougall, I., 1992. Stratigraphy of the Lothidok range, northern Kenya, and K/Ar ages of its Miocene primates. J. Hum. Evol. 22, 47–71.
Brown, F.H., Fuller, C.R., 2008. Stratigraphy and tephra of the Kibish Formation, southwestern Ethiopia. J. Hum. Evol. 55 (3), 366–403.
Cerling, T.E., 2014. Stable isotope evidence for hominin environments in Africa. In: In: Cerling, T.E. (Ed.), Treatise on Geochemistry, vol 14. Archaeology and anthropology, Oxford, Pergamon, pp. 157–167.
Cerling, T.E., Quade, J., 1993. Stable carbon and oxygen isotopes in soil carbonates. In: Swart, P.K., Lohmann, K.C., Mckenzie, J., Savin, S. (Eds.), Climate Change in Continental Isotopic Records. American Geophysical Union, Washington, D.C, pp. 217–231.
Cerling, T.E., Wynn, J.G., Andanje, S.A., Bird, M.I., Korir, D.K., Levin, N.E., Mace, W., Macharia, A.N., Quade, J., Remien, C.H., 2011. Woody cover and hominin environments in the past 6 million years. Nature 476 (7358), 51–56.
Chritz, K.L., Cerling, T.E., Freeman, K.H., Hildebrand, E.A., Janzen, A., Prendergast, M.E., 2019. Climate, ecology and the spread of herding in eastern Africa. Quat. Sci. Rev. 204, 119–132.
Cuthbert, M.O., Gleeson, T., Reynolds, S.C., Bennett, M.R., Newton, A.C., McCormack, C.J., Ashley, G.M., 2017. Modelling the role of groundwater hydro-refugia in East African hominin evolution and dispersal. Nat. Commun. 8, 15696.
Feibel, Craig S., 2011. A geological history of the Turkana Basin. Evol. Anthropol. Issues News Rev. 20 (6), 206–216.
Foerster, V., Vogelsang, R., Junginger, A., Asrat, A., Lamb, H.F., Schaebitz, F., Trauth, M.H., 2015. Environmental change and human occupation of southern Ethiopia and northern Kenya during the last 20,000 years. Quat. Sci. Rev. 129, 333–340.
Garcin, Y., Melnick, D., Strecker, M.R., Olago, D., Tiercelin, J.-J., 2012. East African mid-Holocene wet–dry transition recorded in palaeo-shorelines of Lake Turkana, northern Kenya Rift. Earth Planet. Sci. Lett. 331–332, 322–334.
Goldstein, S., Hildebrand, E., Storozum, M., Sawchuk, E., Lewis, J., Ngugi, C., Robbins, L.H., 2017. New archaeological investigations at the Lothagam harpoon site at Lake Turkana. Antiquity 91 (360).
Haberyan, K.A., Hecky, R.E., 1987. The late Pleistocene and Holocene stratigraphy and paleolimnology of lakes Kivu and Tanganyika. Palaeogeogr. Palaeoclimatol. Palaeoecol. 61 (3–4), 169–197.
Hilgen, F.J., 1991. Astronomical calibration of Gauss to Matuyama sapropels in the Mediterranean and implication for the geomagnetic palarity time scale. Earth Planet. Sci. Lett. 104, 226–244.
Jones, M.B., 1988. Photosynthetic responses of C3 and C4 wetland species in a tropical swamp. J. Ecol. 76, 253–262.
Kilham, P., 1990. Ecology of Melosira species in the great lakes of Africa. In: Tilzer, M.M., Serruya, C. (Eds.), Large Lakes: Ecological Structure and Function. Springer-Verlag, Berlin, pp. 415–427.
Klaus, K.E., Neuendorf, J.P., Mehl, J., Jackson, J.A., 2005. Glossary of Geology. American Geological Institute, Alexandria, VA, pp. 800.
Kutzbach, J.E., 1981. Monsoon climate of the early Holocene: climate experiment with the earth's orbital parameters for 9000 Years ago. Science 214 (4516), 59–61.
Kutzbach, J.E., Liu, Z., 1997. Response of the African monsoon to orbital forcing and ocean feedbacks in the middle Holocene. Science 278, 440–443.
LacCore, N.L.C.F., 2013. Loss-on-ignition Standard Operating Procedure. pp. 1–5.
Levin, N.E., Brown, F.H., Behrensmeyer, A.K., Bobe, R., Cerling, T.E., 2011. Paleosol carbonates from the omo group: isotopic records of local and regional environmental change in East Africa. Palaeogeogr. Palaeoclimatol. Palaeoecol. 307 (1–4), 75–89.
Mantlana, K., Arneth, A., Veenendaal, E., Wohland, P., Wolski, P., Kolle, O., Wagner, M., Lloyd, J., 2008. Photosynthetic properties of C4 plants growing in an African savanna/wetland mosaic. J. Exp. Bot. 59 (14), 3941–3952.
Marean, C.W., 2011. Coastal South Africa and the coevolution of the modern human lineage and the coastal adaptation. In: Bicho, N.F., Haws, J.A., Davis, L.G. (Eds.), Trekking the Shore: Changing Coastlines and the Antiquity of Coastal Settlement. Springer, pp. 421–440.
Melnick, D., Garcin, Y., Quinteros, J., Strecker, M.R., Olago, D., Tiercelin, J.-J., 2012. Steady rifting in northern Kenya inferred from deformed Holocene lake shorelines of the Suguta and Turkana basins. Earth Planet. Sci. Lett. 331–332, 335–346.
Michel, L.A., Driese, S.G., Nordt, L.C., Breecker, D.O., Labotka, D.M., Dworkin, S.I., 2013. Stable-isotope geochemistry of vertisols formed on marine limestone and implications for deep-time paleoenvironmental reconstructions. J. Sediment. Res. 83 (4), 300–308.
Mirazon Lahr, M., Rivera, F., Power, R.K., Mounier, A., Copsey, B., Crivellaro, F., Edung, J.E., Maillo Fernandez, J.M., Kiarie, C., Lawrence, J., Leakey, A., Mbua, E., Miller, H., Muigai, A., Mukhongo, D.M., Van Baelen, A., Wood, R., Schwenninger, J.L., Grun, R., Achyuthan, H., Wilshaw, A., Foley, R.A., 2016. Inter-group violence among early Holocene hunter-gatherers of West Turkana, Kenya. Nature 529 (7586), 394–398.
Morrissey, A., Scholz, C.A., 2014. Paleohydrology of lake Turkana and its influence on the nile river system. Palaeogeogr. Palaeoclimatol. Palaeoecol. 403, 88–100.
Nicholson, S.E., 1996. A review of climate dynamics and climate variability in Eastern Africa. In: Johnson, T.C., Odada, E.O. (Eds.), The Limnology, Climatology and Paleoclimatology of the East African Lakes. Gordon and Breach Publishers, pp. 25–56.
Nordt, L.C., Driese, S.D., 2009. Hydropedological model of vertisol formation along the Gulf Coast Prairie land resource area of Texas. Hydrol. Earth Syst. Sci. 13, 2039–2053.
Owen, R.B., Renaut, R.W., 1986. Sedimentology, stratigraphy and palaeoenvironments of the Holocene Galana Boi Formation, NE lake Turkana, Kenya. In: In: Frostick, L.E., Renaut, R.W., Reid, I., Tiercelin, J.J. (Eds.), Sedimentation in the African Rifts Volume No. 25. Geological Society Special Publications Blackwell Scientific Publications, pp. 311–322.
Owen, R.B., Utha-aroon, C., 1999. Diatomaceous sedimentation in the tertiary Lampang basin, northern Thailand. J. Paleolimnol. 22, 81–95.
Owen, R.B., Barthelme, J.W., Renaut, R.W., Vincens, A., 1982. Palaeolimnology and archaeology of Holocene deposits north-east of lake Turkana, Kenya. Nature 298, 523–528.
Popkin, B.M., D'Anci, K.E., Rosenberg, I.H., 2010. Water, hydration, and health. Nutr. Rev. 68 (8), 439–458.
Prendergast, M.E., Beyin, A., 2018. Fishing in a fluctuating landscape: terminal Pleistocene and early Holocene subsistence strategies in the Lake Turkana Basin, Kenya. Quat. Int. 471, 203–218.
Prendergast, M.E., Lane, P.J., 2010. Middle Holocene fishing strategies in East Africa: zooarchaeological analysis of Pundo, a Kansyore shell midden in northern Nyanza (Kenya). Int. J. Osteoarchaeol. 88–112.
Reimer, P.J., Bard, E., Bayliss, A., Beck, J.W., Blackwell, P.G., Ramsey, C.B., Buck, C.E., Cheng, H., Edwards, R.L., Friedrich, M., Grootes, P.M., Guilderson, T.P., Haflidason, H., Hajdas, I., Hatté, C., Heaton, T.J., Hoffmann, D.L., Hogg, A.G., Hughen, K.A., Kaiser, K.F., Kromer, B., Manning, S.W., Niu, M., Reimer, R.W., Richards, D.A., Scott, E.M., Southon, J.R., Staff, R.A., Turney, C.S.M., Plicht, J. v. d., 2013. IntCal13 and Marine13 radiocarbon age calibration curves 0-50,000 years cal BP. Radiocarbon 55 (2), 1869–1887.
Robbins, Lawrence H., 1974. The Lothagam site: A late stone age fishing settlement in the Lake Rudolph basin, Kenya. Anthropological Series 1 (2) East Lansing: Michigan State University.
Robbins, L.H., 1975. Bone artefacts from The lake Rudolf basin. East Afr.: Curr. Anthropol. 16, 632–633.
Ryves, D.B., Battarbee, R.W., Fritz, S.C., 2009. The dilemma of disappearing diatoms: Incorporating diatom dissolution data into palaeoenvironmental modelling and reconstruction. Quat. Sci. Rev. 28, 120–136. https://doi.org/10.1016/j.quascirev.2008.08.021.
Scholz, C.A., King, J.W., Ellis, G.S., Swart, P.K., Colman, S.M., 2003. Paleolimnology of lake Tanganyika, East Africa, over the past 100 k yr. J. Paleolimnol. 30, 139–150.
Shanahan, T.M., McKay, N.P., Hughen, K.A., Overpeck, J.T., Otto-Bliesner, B., Heil, C.W., King, J., Scholz, C.A., Peck, J., 2015. The time-transgressive termination of the African Humid Period. Nat. Geosci. 8 (2), 140–144.
Stewart, K.M., 1991. Modern fishbone assemblages at Lake Turkana, Kenya: a method to aid in recognition of hominin fish utilization. J. Archaeol. Sci. 18, 579–603.
Stone, J.R., Cohen, A.S., Westover, K.S., 2011. Late Pleistocene paleohydrography and diatom paleoecology of the central basin of Lake Malawi, Africa. Palaeogeogr. Palaeoclimatol. Palaeoecol. 303, 51–70.
Talma, A.S., Vogel, J.C., 1993. A simplified approach to calibrating 14C dates. Radiocarbon 35 (2), 317–322.
Targulian, V.O., Krasilnikov, P.V., 2007. Soil system and pedogenic processes: self-

organization, time scales, and environmental significance. Catena 71, 373–381. https://doi.org/10.1016/j.catena.2007.03.007.
van der Lubbe, H.J.L., Krause-Nehring, J., Junginger, A., Garcin, Y., Joordens, J.C.A., Davies, G.R., Beck, C., Feibel, C.S., Johnson, T.C., Vonhof, H.B., 2017. Gradual or abrupt? Changes in water source of lake Turkana (Kenya) during the African Humid Period inferred from Sr isotope ratios. Quat. Sci. Rev. 174, 1–12.
Vigliotti, L., Asioli, A., Bergami, C., Capotondi, L., Piva, A., 2011. Magnetic properties of the youngest sapropel S1 in the Ionian and Adriatic Sea: inference for the timing and mechanism of sapropel formation. Ital. J. Geosci. 130 (1), 106–118.
White, F., 1983. The Vegetation of Africa, a Descriptive Memoir to Accompany the UNESCO/AETFAT/UNSO Vegetation Map of Africa (3 Plates, Northwestern Africa, Northeastern Africa, and Southern Africa, 1: 5,000,000). Unesco, Paris.
Whitworth, T., 1965a. Artifacts from Turkana, northern Kenya. S. Afr. Archaeol. Bull. 20 (78), 75–78.
Whitworth, T., 1965b. The Pleistocene lake beds of Kabua, northern Kenya. Durh. Univ. J. 57, 88–100.
Wilson, C., 2016. Reconstructing Paleoenvironment Using Soil Carbonate Isotopic Data from the Holocene Galana Boi Formation. Hamilton College, Turkana, Kenya [B.A.].
Wright, D.K., Forman, S.L., Kiura, P.W., Bloszies, C., Beyin, A., 2015. Lakeside view: socio-cultural responses to changing water levels of Lake Turkana, Kenya. Afr. Archaeol. Rev. 32, 335–367.
Yuretich, R.F., 1979. Modern sediments and sedimentary processes in lake Rudolf (lake Turkana) eastern Rift valley, Kenya. Sedimentology 26, 313–331.
Yuretich, R.F., Cerling, T.E., 1983. Hydrogeochemistry of Lake Turkana, Kenya: mass balance and mineral reactions in an alkaline lake. Geochem. Cosmochim. Acta 47, 1099–1109.